ISSN: 2754-4915

Journal of Material Sciences & Manufacturing Research

SCIENTIFIC Research and Community

Review Article

Open Access

Studies on Multifunctional Nanostructured Materials

Nabanita Dutta[1], Bandyopadhyay SK[2*], Subhasis Rana[3], Pintu Sen[4] and Himanshu AK[5]

[1]PhD Lead Engineer at Vestas Technology R&D Chennai, India

[2]Meghnad Saha Institute of Technology, India

[3]Department of Basic Science and Humanities, Institute of Engineering and Management, University of Engineering and Management, Kolkata-700160, India

[4]Variable Energy Cyclotron Centre,1/AF, Bidhan Nagar, Kolkata-700 064, India

ABSTRACT

Multifunctional materials are of today's quest. Miniaturization, i.e. development of these materials in the form of nanomaterials is of primary need considering their application in devices. Moreover, if these are obtained in nanostructured form, they can bring wonders.

We have adopted a method for developing multiferroic BiFeO3 (BFO) with simultaneous antiferromagnetic, ferroelectric & ferroelastic behaviour in form of nanostructures like nanorods, nanowire etc. by employing Anodised Alumina (AAO) template with various pore sizes from 20nm with solution route followed by controlled vacuum filtration and sintering. Diameters of nanorods are in the range of 20-100 nm as observed by FESEM. Capacitance assayed by cyclic voltammetry (CV) and charge discharge processes reveals a very high value of specific capacitance of 450F/gm. Capacitance has been estimated by extrapolating the charge collected at the electrode to that at scanning rate of infinity which is relevant for the charge collected at the nanorods protruding out of the template. Charging and discharging times are quite constant over a large number of cycles. This large value of specific capacitance can be attributed to the nanostructure form of BFO nanorod. The high value of specific capacitance of BFO nanorods brings forth its use as electrode in storage energy devices. Also, a high value of polarization as well as a significant magnetic susceptibility are observed in multiferroic Bismuth Ferrite (BFO) in the form of nanorods protruding out. The high values of polarization and magnetic susceptibility are attributed to the structured form of BFO nanorods giving rise to the directionality. There is no leakage current in P-E loop examined at various fields and frequencies. Magnetocapacitance measurements reflect a significant enhancement in magnetoelectric coupling also.

***Corresponding author**

Bandyopadhyay SK, Meghnad Saha Institute of Technology, India.

Received: March 07, 2025; **Accepted:** March 12, 2025; **Published:** March 19, 2025

Introduction

Electrochemical Capacitors (EC), popularly known as supercapacitors provide high power and long cycle life, essential for energy storage devices. They are categorized as electrochemical double layer capacitors (EDLC) and pseudocapacitors. In EDLC, capacitance originates in the charge separation at the electrode-electrolyte interface, whereas pseudocapacitance arises from fast, reversible faradaic redox reactions taking place on or near the surface of the electrode [1]. Electrochemical performances of a material as electrode can be assayed by cyclic voltammetry and galvanostatic charge-discharge studies of specific capacitance. An electrode is judged by its capacitance value and the number of charge-discharge cycles it withstands, maintaining the constancy of capacitance. This brings forth the search for a wide variety of materials. In general, transition metal oxides like RuO2, MnO2 etc. show high specific capacitance with their redox behavior.

In this context, it is quite interesting to study the capacitance of multifunctional materials like the multiferroic Bismuth ferrite (BFO) showing coexistence of ferroelectricity as well as antiferromagnetism with wide applications [2]. Lokhande et al. observed specific capacitance value of 81F/gm in BFO films [3]. Attempts have been made to obtain BFO in 1-Dimensional nanostructure forms like nanowire, nanorod, etc. [4,5]. The nanostructured forms can be expected to offer better efficiency owing to large surface area giving rise to a high value of specific capacitance, for example in α-MnMoO4 nanorods [6]. This prompted us to study the capacitance of BFO nanostructure with its redox behaviour.

In this letter, we report the development of BFO nanorod by the wet chemical template assisted method and its capacitance studies by electrochemical means. We have evaluated specific capacitance both through cyclic voltammetry at different scanning rates and charge-discharge studies galvanostatically employing different currents. To our knowledge, there has not been any study of BFO nanorod in this respect so far.

Experimental Details

AAO templates of 60 μm thickness and 13 mm diameter with pore size distribution ranges from 20-100 nm were employed. 0.1M solutions of Bi(NO3)3 and Fe(NO3)3 were prepared with stoichiometric amounts of the nitrates using methoxymethanol as solvent with pH adjusted to 2-3. The filling of nanopores was achieved by the directional flow of the ions in the template adopting the controlled vacuum technique. The templates with

pores containing solution were sintered for 3 hours at 7500C to get the required phase without unwanted grain growth. We attempted controlled etching process with 1M NaOH and the bundle of nanowires and nanorods emerged. Weights of BFO nanorods measured using a very sensitive microbalance (resolution of 1μgm) by subtracting the weights of respective AAO were in the range 80-100μg.

The nanowires and nanorods were examined by FEI Scanning Electron Microscope (SEM) with a resolution of 6nm aided by Energy Dispersive X-Ray (EDX) for compositional analysis. Transmission electron microscopy (TEM) was done by high resolution TEM (Model: FEI T20 with applied voltage of 200KV). Selective Area Electron Diffraction (SAED) was also undertaken to ascertain crystal structure of the nanorods.

Cyclic Voltammetry (CV) and galvanostatic charge-discharge were studied with AUTOLAB-30 potentiostat/galvanostat for both BFO on AAO and AAO blank templates being used as electrodes. The half etched templates used in SEM were employed for this purpose with the protrusion length of 1μm (as visible by SEM) over the template of thickness 60μm. Electrodes were prepared by connecting Cu lids with AAO/BFO templates through conducting silver paste. All the electrochemical experiments (i.e CV, Charge-discharge) were performed with two-electrode system having identical electrodes with respect to shape, size and made of same active electrode materials (i.e. Type-I symmetric supercapacitor) using an electrolyte containing 1M Na_2SO_4 in water. A platinum electrode and a saturated Ag/AgCl electrode were used as counter and reference electrodes respectively. All the CVs were measured between -0.6 to +0.6 V (i.e. operating window of 1.2V) with respect to reference electrode at different scan rates (5mV/s to 50mV/s). Constant currents ranging from 15 to 30 μAmp have been employed for charging/discharging the cell in the voltage range from -0.6 to +0.6 V.

In a symmetrical system where the active material weight is the same for the two electrodes,

$$C_s = \frac{2C}{m} \quad (1)$$

where m is the active mass of the single electrode, C is the discharge capacitance and C_s is the specific capacitance of the electrode [7]. The charge accumulated on BFO was assayed by subtracting the charge on blank AAO from that on BFO/AAO electrode. We have applied several cycles of CV as well as charge-discharge to study the stability of the system with cycling.

Results and Discussions

There are two kinds of 1D nanostructure in the form of nanowires as well as nanorods as apparent from figures. 1a and 1b similar to earlier groups [4,5]. Figure. 1a shows the bundles of nanowires and nanorods which have come out after etching the template with NaOH. Basically they are nanorods but we observed them in the form of a bundle after etching. There is a distribution in diameters of nanorods as revealed in figure. 1a. Cross sectional view is showing development of nanorods in Figure. 1b- a representative case. It demonstrates the structures of several nanorods (around 20 in a region of 5 μm x 5 μm) with high aspect ratio protruding out of the pores after partial etching. The compositional analysis was performed by EDX analysis at different nanorods and they reflected Bi:Fe atomic ratios of slightly more than 1:1 reflecting a little more Bi content with a fluctuation within 3 per cent. Figure. 1c shows the TEM picture of nanorods of high density with intact structure. The inset indicates a clear SAED pattern with prominent rings signifying the development of polycrystalline BFO.

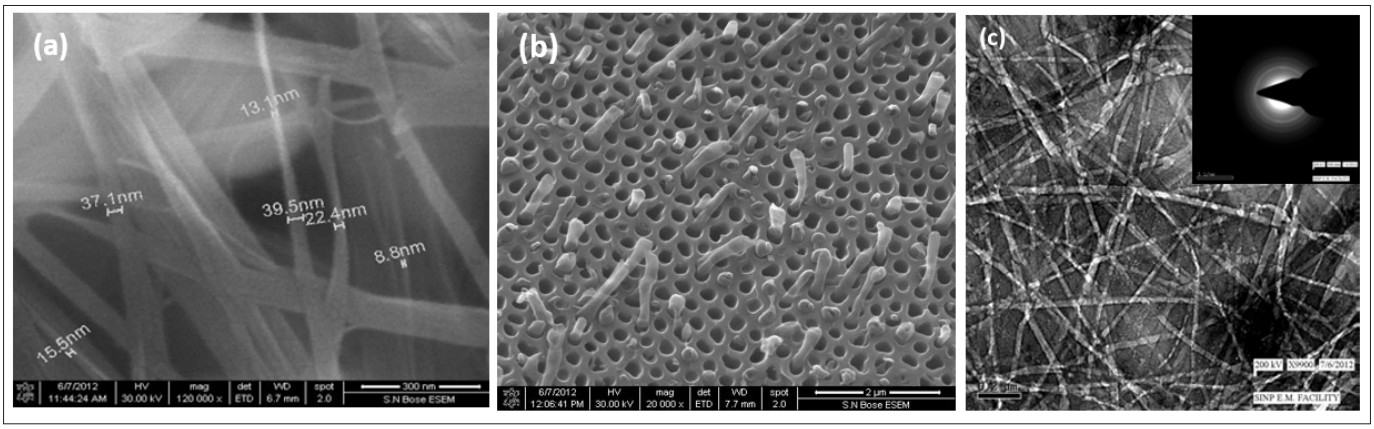

Figure 1(a): SEM Showing Bundles of Nanorod, **(b)** SEM of Nanorod Protruding from Pores and **(c)** TEM of BFO Nanorods and Corresponding SAED Pattern Shown in the Inset

Figure.2 displays the XRD pattern of BFO nanorods along with AAO template. The dominant peaks correspond to AAO having the maximum amount. But there is a distinct BFO characteristic peak corresponding to 110 plane. This is quite appreciable considering very small amount of BFO (around 0.5% of the wt. of the template).

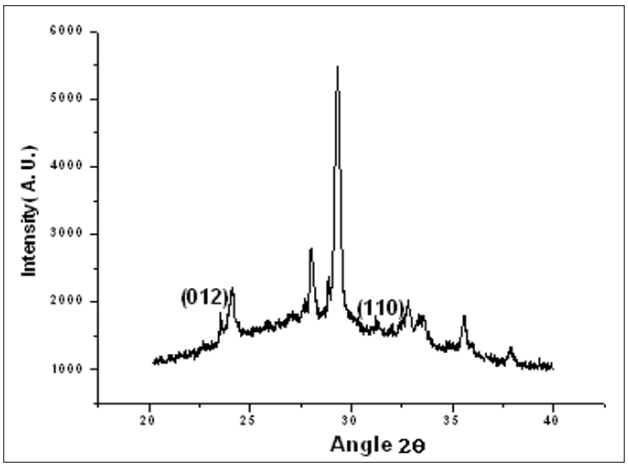

Figure 2: XRD Pattern of BFO along with AAO Template. Characteristic Peak Corresponding to 110 Plane is Noticed Even with Small Amoit of BFO Compared to the Template

Pseudocapacitance

Typical cyclic voltammograms (CV) of different samples at a scan rate of 50 and 10mV/s between -0.6 and 0.6V in aqueous solution of 1M Na2SO4 are shown in Figure. 3a. Cyclic voltammograms of different samples are quite symmetrical with a mirror image of the current response from voltage, indicating ideal pseudocapacitative behavior and excellent reversibility in charging and discharging at a constant rate over the voltage range of –0.6 to 0.6V [8]. Voltammetric charges (q*) at different potential scan rate v (mV/s) were obtained by integration of the voltammetric curves followed by division with the geometric surface area of the samples without correction for background capacitative current. The charge accumulation on BFO/AAO and AAO individually assayed by CV established that the contribution from AAO was significantly less than BFO/AAO for same weight. Typical values were 2.270x10-3 Coulombs for BFO/AAO and 6.45x10-4 Coulombs for AAO at the scanning rate of 20mv/sec.

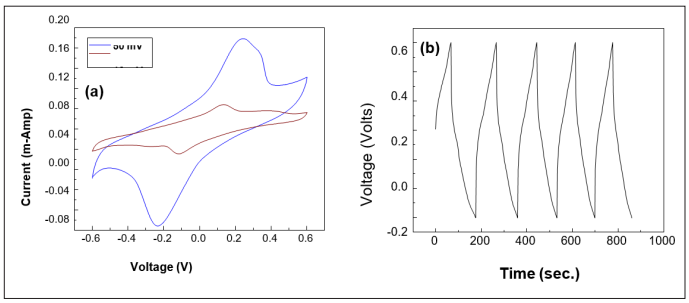

Figure 3(a): Cyclic Voltammogram of BFO on AAO at Different Scan Rates and (b) Charge-Discharge Cycle of BFO on AAO Template at 30µAmp Current.

Let us now try to understand the charge distribution in BFO/AAO template network. Our system consists of BFO nanorods some of them protruding out of pores along with porous AAO template with pore sizes varying from 20-100nm. Total charge will be distributed as inner charge in the pores (some of which contains BFO) and as outer charge on the BFO nanorods protruding 1 µm on the average above the surface of the template. Around half of the pores filled by BFO have protruded nanorods; others are inside the pores. The depth of the pores is 60µm– the thickness of the template. Thus, the protruded portion of BFO– solely responsible for the contribution to q* is 1/60 of the wt. of protruded BFO nanorod which itself is half of the total wt. 80µgms of BFO. Rest is embedded in pores. q* (obtained by extrapolating the plot of charge q* vs. $v^{-1/2}$ to $v^{-1/2}$ =0 and taking the intercept) is $1.50x10^{-4}$ coulombs. On this basis, the specific capacitance of BFO nanorod structure comes out to be 450 F/gm. This large value of specific capacitance can be attributed to the nanostructure form of BFO nanorod.

The pseudocapacitative behavior of BFO stems from its redox reaction. $BiFeO_3$ is more readily reduced than oxidised, with the creation of oxygen vacancies and Fe^{2+} species. The highly unfavourable energy (> 4 eV) estimated for disproportionation of Fe^{3+} (to Fe^{2+} and Fe^{4+}) suggests that tetravalent iron ions are unlikely to form in this material through this process.

Polarisation

Figure 4 shows the P-E loops of BFO nanorod on AAO template at various frequencies from 90 Hz to 400 Hz. The hysteresis loops are quite appreciable characteristic of a ferroelectric material decreasing with increasing frequency. We have also examined the blank AAO templates which did not display any P-E loop but rather noise. Hence the P-E loop and the polarization values observed here at different frequencies are due to the contribution of BFO only. We have not noticed any saturation up to the applied field of 60KV/cm. The gap in the plot is seen due to improper depolarization. The ferroelectricity of BFO originates from the relative displacements of Bi and O ion induced by $6s^2$ lone pair of electron that resulting a net polarization. Such polarization is an example of orientaional polarization which is very much affected by distribution of the polarization domains specifically upon their directionality.

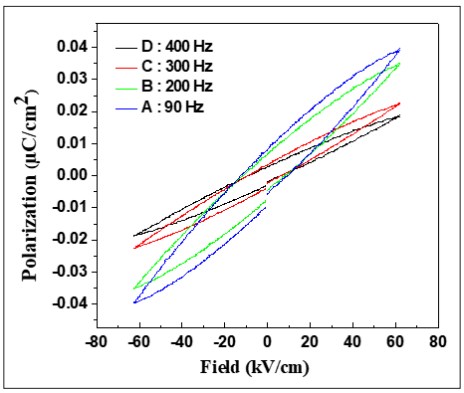

Figure 4: Ferroelectric Hysteresis Loops of BFO Nanorod at Various Frequencies

Relatively low value of polarization is characteristic of nanoparticles as observed by us earlier [9]. However, it is quite high in epitaxial BFO films and BFO single crystals where the projection of polarization takes the orientation along the easy axis of growth crystals where net polarization matches along the direction of growth basically along (1 1 1) plane [10,11]. Most significantly, the observed polarization of BFO nanorods is remarkably high (~0.04µC/cm²) if the polarization is normalized by the weight of the nanorods which is 80 micrograms only. The value is comparable to our earlier results on agglomerated BFO nanoparticles of wt. of ~80mg. This high value of polarization can be attributed to the directional growth of BFO as rod structure. The directional growth guided by the cylindrical pore structure has also prevented the development of grain boundaries. We have employed a moderate sintering time to avoid the grain growth. Moreover, preheated furnace was taken up to get rid of the loss of Bismuth which helped maintaining Bismuth to Iron ratio nearly 1:1 which was varied through EDX studies.

There is no leakage current (indicated by decrease in polarization with electric field) associated with our nano rods. The leakage current is observed mainly in a grain boundary region due to the accumulation of defects and these defects appear from oxygen vacancies as well as metallic impurities like Bi^{2+}, iron oxide etc. This indicates that our BFO nanorod is free from oxygen vacancies and other impurities.

We have also investigated the magnetocapacitance of BFO Nanorod (Figure. 5) as a function of magnetic field which is also quite appreciable considering the wt. of BFO nanorod. Magnetocapacitance is a measure of magnetoelectric coupling in a multiferroic system.

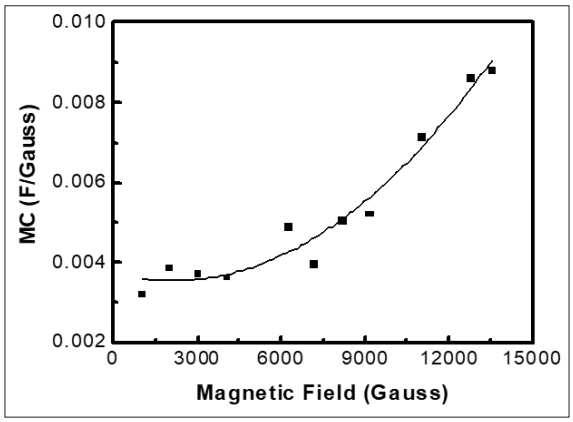

Figure 5: Magnetocapacitance of BFO Nanorod at Various Magnetic Fields

Conclusion

We have studied capacitance and other multiferroic properties like polarization, magentocapacitance of BFO nanorods developed on AAO templates by electrochemical means. Capacitance of AAO as evaluated by accumulated charge is significantly less as compared to BFO. BFO nanorods protruded from the template surface demonstrated a very high specific capacitance of 450F/gm as measured from the charge accumulated on the outer surface. The high specific capacitance is due to the particular nanostructure in the form of the rod. There is a close resemblance between the capacitance assayed by CV and charge-discharge methods. The system is quite stable with respect to repeated cycling. BFO system undergoes a redox process with O vacancies being generated giving rise to pseudocapacitative behavior with high specific capacitance. The high specific capacitance in the nanorod structure coupled with stability at long cycles brings forth its application as electrodes in batteries. The polarization values as observed from plot against electric fields at various frequencies are also quite appreciable considering the small wt of BFO nanorod. Magnetocapacitance values also signify quite high magnetoelectric coupling rendering the use of BFO nanorod in various magnetoelecric devices [12,13].

Acknowledgements

Authors gratefully acknowledge Dr. P.K.Mukhopadhyay and Mr. Sakti Nath Das of S.N.Bose Center for basic Sciences for SEM studies and Mr. Pulak Kumar Roy of Saha Instititute of Nuclear Physics for TEM studies.

References

1. Zhang Y, Feng H, Wu X, Wang L, Zhang A, et al. (2009) Progress of electrochemical capacitor electrode materials: A review. International Journal of Hydrogen Energy 34: 4889-4899.
2. Zhang XY, Lai CW, Zhao X, Wang DY, Dai JY (2005) Synthesis and ferroelectric properties of multiferroic BiFeO3 nanotube arrays. Appl Phys Lett 87: 143102-143104.
3. Lokhande CD, Gujar TP, Shinde UR, Mane RS, Han SH (2007) Electrochemical supercapacitor application of pervoskite thin films. Electrochem Comm 9: 1805-1807.
4. Gao F, Yuan Y, Wing KF, Chen XY, Chen F, et al. (2006) Preparation and photoabsorption characterization of BiFeO3 nanowires. Appl Phys Lett 89: 102506-102508.
5. Xie SH, Li JY, Proksch R, Liu YM, Zhou YC, et al. (2008) Nanocrystalline multiferroic BiFeO3 ultrafine fibers by sol-gel based electrospinning. Appl Phys Lett 93: 222904-222906.
6. Purusothaman KK, Cuba M, Muralidharan (2012) Supercapacitor behavior of α- MnMoO4 nanorods on different electrolytes. G Mat Res Bull 47: 3348-3351.
7. Portet C, Taberna PL, Simon P, Laberty-Robert C (2004) Modification of Al current collector surface by sol–gel deposit for carbon–carbon supercapacitor applications. Electrochim Acta 49: 905-912.
8. Reddy RN, Reddy RG (2003) Sol–gel MnO2 as an electrode material for electrochemical capacitors. J Power Source 124: 330-337.
9. Nabanita Dutta, Bandyopadhyay SK, Himanshu AK, Pintu Sen, Sangam Banerjee, et al. (2013) Ferroelectric and Magnetic Properties of Agglomerated Bismuth Ferrite Nanoparticles. Advanced Science, Engineering and Medicine 5: 979-983.
10. Lebeugle D, Colson D, Forget A, Viret M, Bonville P, et al. (2007) Room-temperature coexistence of large electric polarization and magnetic order in Bi Fe O3 single crystals. Phys Rev B 76: 024116.
11. Li J, Wang J, Wuttig M, Ramesh R, Wang N, et al. (2004) Dramatically enhanced polarization in (001), (101) and (111) Bi Fe O3 thin films due to epitiaxial-induced transitions. Appl Phys Lett 84: 5261-5263.
12. Burke LD, Murphy OJ (1979) Cyclic voltammetry as a technique for determining the surface area of RuO2 electrodes. J Electroanal Chem 96: 19-27.
13. Ardizzone S, Fregonara G, Trasatti S (1990) "Inner" and "outer" active surface of RuO2 electrodes. Electrochem Acta 35: 263-267.